

Conference paper

Sandra L. Orellana, Annesi Giacaman, Alejandra Vidal, Carlos Morales, Felipe Oyarzun-Ampuero, Judit G. Lisoni, Carla Henríquez-Báez, Luis Morán-Trujillo, Miguel Concha and Ignacio Moreno-Villoslada*

Chitosan/chondroitin sulfate aerogels with high polymeric electroneutralization degree: formation and mechanical properties

<https://doi.org/10.1515/pac-2016-1111>

Abstract: The formation of ultralight, highly porous solid materials (porosity higher than 99 %) containing equivalent molar amounts of chitosan (CS) and chondroitin sulfate (ChS) is presented. First, we show protocols to produce colloidal suspensions of assembled polymer nanocomplexes by simultaneously mixing equimolar amounts of the oppositely charged polysaccharides, preventing macroprecipitation. The colloidal suspensions were then freeze-dried to form the active aerogels. Apparent density in the order of 10^0 – 10^1 mg/cm³ was achieved. The materials show low stiffness (Young's modulus of about 2 kPa), which make them easy to handle for clinical applications, and easy to compress, pack, store and transport. These characteristics promote them as cheap, safe and biodegradable materials able to be used for several therapeutic purposes, such as wound healing.

Keywords: aerogels; biocompatible materials; colloidal suspensions; ICC-13; mechanical properties; polysaccharides.

Introduction

Polysaccharide-based aerogels are sustainable materials that can be used in several medical applications demanding biodegradability [1, 2]. These are highly porous materials of extremely low density whose fabrication involves the preparation of a gel from an aqueous solution, and subsequent removal of the solvent, arising a material that almost maintains the volume of the original gel. The gel is obtained by physical or chemical cross-linking [3, 4]. Physical hydrogels are formed upon thermal, ionic, or pH-induced gelations, making use of supramolecular interactions between the gel components, avoiding the formation of new covalent bonds. Chemical hydrogels can be prepared through chemical cross-linking by adding cross-linkers able to promote

Article note: A collection of invited papers based on presentations at the 12th Conference of the European Chitin Society (12th EUCHIS)/13th International Conference on Chitin and Chitosan (13th ICC), Münster, Germany, 30 August–2 September 2015.

***Corresponding author: Ignacio Moreno-Villoslada**, Instituto de Ciencias Químicas, Facultad de Ciencias, Universidad Austral de Chile, Isla Teja, Casilla 567, Valdivia, Chile, Tel.: +56 63 2293520, E-mail: imorenovilloslada@uach.cl

Sandra L. Orellana, Carlos Morales and Luis Morán-Trujillo: Instituto de Ciencias Químicas, Facultad de Ciencias, Universidad Austral de Chile, Valdivia, Chile

Annesi Giacaman, Alejandra Vidal and Miguel Concha: Instituto de Anatomía, Histología y Patología, Facultad de Medicina, Universidad Austral de Chile, Valdivia, Chile

Felipe Oyarzun-Ampuero: Department of Sciences and Pharmaceutical Technologies, Universidad de Chile, Santiago, Chile

Judit G. Lisoni and Carla Henríquez-Báez: Instituto de Ciencias Físicas y Matemáticas, Facultad de Ciencias, Universidad Austral de Chile, Valdivia, Chile

covalent bonding between polysaccharide chains. Although chemical cross-linking allows a better control of the porous structure when compared to physical hydrogels, synthetic efforts and loss of biocompatibility are drawbacks of aerogels produced from chemically cross-linked hydrogels for medical applications.

Scaffolds and sponges for tissue engineering are typically prepared with densities in the order of magnitude of 10^2 mg/cm³ or higher [5, 6]. The strategy underlining the design of these materials is to provide a porous reinforced matrix where cells can attach and grow to build up the regenerated tissue [7–9]. However, facing the problem of healing chronic wounds, such as diabetic foot and venous ulcers, a first hypothesis arose: the material to be applied as wound healing inductor should be a non-toxic, biodegradable, resorbable, and, importantly, ultralight porous material so that the amount of matter to be applied to the wound is minimized, avoiding additional metabolic stress to the wounds, impairing healing and production of excessive debris and other by-products of metabolism. Thus, aerogels with density ranging between 10^0 and 10^1 mg/cm³ should constitute adequate materials.

Such low density may generate materials with poor mechanical properties, so the first hypothesis led us to the second hypothesis by which the material to be applied as wound healing inductor should be physiologically functional, rather than constitute a scaffold for cell attachment and growing. Thus, bioactive molecules should be chosen for the design of the aerogels. Glycosaminoglycans such as hyaluronic acid, keratan sulfate and chondroitin sulfate (ChS) are good candidates to provide functional properties, since they are part of the extracellular matrix [10–13]. The biopolymer ChS is used in medicine and pharmacology in devices presenting anti-inflammatory and antimicrobial activities [14], and shows activity in cell differentiation and proliferation [15, 16]. It has also been used as a vehicle in pharmacological systems [11]. On the other hand, chitosan (CS) has been used for medical purposes such as improving wound healing [17, 18]. Different derivatives of chitin and CS have been prepared for wound dressing applications in the form of hydrogels, fibers, membranes, scaffolds and sponges [19–22]. The importance of CS in biomaterials is not only due to its biocompatibility and structural properties that it confers to the materials, but also to its biological properties [17]. The properties of both ChS and CS polymers may be combined in single materials, and, thus, CS/ChS biomaterials have been evaluated in tissue engineering such as bone and cartilage regeneration [23, 24].

Highly charged molecules and nanostructures applied to damaged tissues may produce disruption of the cellular membrane integrity, and induce extensive inflammatory response [25]. Studies on proliferation of fibroblasts in sponges containing a high excess of negative polymeric charges show low rate of cellular growth, but upon neutralization with the cationic polysaccharide CS cell proliferation is stimulated [26]. Thus, a third important hypothesis arose, by which the material to be applied as wound healing inductor should provide almost equivalent amounts of polymeric charges. Due to the large amount of charges of opposite sign that ChS and CS bear, they interact by electrostatic forces, tending to precipitate [27, 28]. Classical methods of formation of porous materials and films based on CS and containing ChS involve excess of CS, and/or preformation of a solid material based on CS, usually through covalently cross-linking [29], and subsequent incorporation of ChS [30, 31]. Other interesting methodologies involve the formation of precipitates of CS/ChS complexes, and further swelling with water at different pHs [28, 32], or direct casting of mixtures of both components to produce films [33]. Interestingly, the electrostatic binding of both cationic and anionic polymers may be considered an out-of-equilibrium process: once the highly charged molecules bind each other, they do not detach, although the molecular chains may undergo slow rearrangement upon changing environmental conditions [28]. Thus, the methodology by which the ionic reactants are mixed is crucial in the final result, so that mixing procedures could hypothetically be achieved that lead to colloidal suspensions of both polysaccharides, avoiding macroprecipitation, from which aerogels may be formed.

Based on all these considerations, in this paper we show the synthesis of ultralight, highly porous CS/ChS aerogels with density ranging in the order of 10^0 – 10^1 mg/cm³ using equimolar amounts of both polysaccharide charges, thus highly neutralized. The formation of colloidal suspensions of CS/ChS nanocomplexes at a molar charge ratio near 1/1 has been developed, avoiding macroprecipitation, prior to freeze-drying to form the solid materials. The materials have the advantage of an easy and low-cost production, avoiding the use of organic solvents or covalent cross-linking reactions. The colloidal suspensions are studied by dynamic light scattering (DLS), and the final solid materials are characterized in terms of swellability, morphology and mechanical properties.

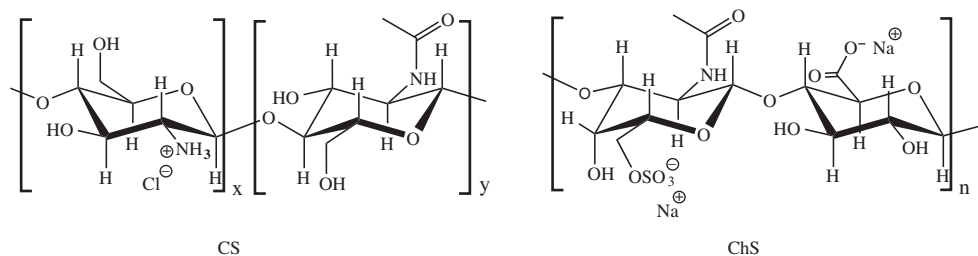


Fig. 1: Molecular structures of CS and ChS.

Experimental

Materials

CS (Protasan™ UP CL 213, Novamatrix, 83 % deacetylation, MW of 239.22 g/mol of amino units considered) and ChS (a sodium salt from bovine trachea, Sigma-Aldrich, MW of 252 g/mol of ionizable groups considered), have been used to prepare the aerogels. The molecular structures are shown in Fig. 1.

Equipment

Solutions were prepared in water deionized in a Simplicity (Millipore) deionizer. The pH of the solutions was measured with a Scholar 425 pH meter (Corning). Apparent size, polydispersity index (PDI) and zeta potential of particles in the resulting CS/ChS colloidal suspensions were measured with a zetasizer Nano ZS equipment (Malvern) with backscatter detection (173°), controlled by the Dispersion Technology Software (DTS 6.2, Malvern). Freeze-drying was carried out in an Alpha 1–2 LD plus lyophilizer (Christ). The obtained materials were characterized by optical microscopy in an Olympus BX43 microscope, and scanning electron microscopy (SEM) in an Inspect 50 microscope (FEI). Other optical pictures were taken with an iPhone 5C mobile phone equipped with an 8 megapixels camera. The mechanical properties were characterized in a CT3 1000 Texture Analyzer (Brookfield) controlled with the TexturePro CT3 software (Brookfield).

Procedures

Stock solutions preparation

CS stock solutions were prepared by dissolving 0.059 g in 25 mL of deionized water previously adjusted to pH 5. Prior to CS stock solution preparation, CS powder was dried in an oven for 4 h at 100 °C, to achieve complete dehydration for accurate weighting, according to provider's suggestions. ChS stock solutions were prepared by dissolving 0.063 g in 25 mL of deionized water. Both polymeric stock solutions were prepared at a concentration of 1×10^{-2} mol of polymeric ionizable groups per liter. The pH spontaneously achieved upon dissolution of the biopolymers was 4.6 and 6.6 for CS and ChS stock solutions, respectively. The pH of deionized water was 5.9.

CS/ChS colloidal suspensions preparation

With the aid of micropipettes, mixtures of CS and ChS were prepared in 50 mL plastic test tubes placing sequentially 3.4 mL of deionized water and different volumes of freshly prepared 1×10^{-2} M stock solutions

Table 1: Volume of the reactants and final concentration to achieve mixtures with different molar fraction of CS and ChS.

X_{ChS}	H ₂ O volume (mL)	ChS volume (mL)	CS volume (mL)	ChS final concentration (M)	CS final concentration (M)
0.2	3.4	0.5	2.1	0.09	0.35
0.3	3.4	0.8	1.8	0.13	0.31
0.4	3.4	1.1	1.6	0.18	0.26
0.5	3.4	1.3	1.3	0.22	0.22
0.55	3.4	1.5	1.2	0.24	0.20
0.6	3.4	1.6	1.1	0.26	0.18
0.7	3.4	1.8	0.8	0.31	0.13

of the respective polysaccharides to achieve a total volume of 6.0 mL with different molar fractions of both components, according to Table 1. Depending on the experiment, the pH of the stock solutions and water was previously adjusted to a determined value by the aid of minimum amounts of HCl and NaOH stock solutions (0.01–1 M). The mixture procedure was assayed following two methods: (A) sequential method: the volume of CS stock solution was firstly added to the test tube containing the 3.4 mL of water, and then the corresponding volume of ChS stock solution was added, under stirring at 20 °C. (B) Simultaneous method: both stock solutions placed in two different micropipettes were added drop wise and simultaneously under stirring at 20 °C. Depending on the polymeric molar fraction of the mixture, the excess of any stock solution was added drop wise at the end. The colloidal suspensions were characterized by analysis of pH, apparent particle size, PDI and zeta potential.

Aerogel formation and characterization

After the colloidal suspensions were formed, series of 2 mL were transferred to wells in 12×8 cm² well-plates of 24 wells. The internal diameters of the wells were 16 mm. The samples were frozen at –15 °C for 24 h, and then freeze-dried at 0.050 mbar for 72 h, and condenser temperature of –57 °C. If necessary, the resulting aerogels were stored at 4 °C in closed containers containing dried silica gel, in order to avoid moisture. Mechanical characterizations of the resulting aerogels were performed in the compression mode, and hardness and apparent Young's modulus (E_{app}) were obtained. The materials were placed on a fixture base table (TA-BT-KIT, Brookfield), and compressed, carefully centered, with a cylindrical TA-10 probe of 12.7 mm of diameter. The resolution of the texture analysis system was 0.1 g and 0.1 mm. The test speed was set at 0.7 mm s⁻¹, the load trigger value ranged from 0.7 to 1.0 g, and the maximum load was set at 12 g. For the final E_{app} analysis, data corresponding to deformations ranging between 30 and 50 % are considered. Porosity threshold of the aerogels was analyzed theoretically after their non-floatability in cyclohexane, a low-dense organic solvent, was corroborated; then, porosity was calculated as (volume of the aerogel – volume of the solid part of the aerogel)/volume of the aerogel.

Results and discussion

Colloidal suspensions

The first challenge of our investigation was the formation of colloidal suspensions of interpolymer nano-complexes of CS and ChS using equimolar amounts of polysaccharide complementary charges. The purpose of using equimolar amounts of CS and ChS charges is to avoid a high electric potential in the final material once it hydrates after application in open wounds. Importantly, as revealed in the literature, biomaterials produce low rate of cellular growth, or even result in cell death, when bearing an excess of polymeric

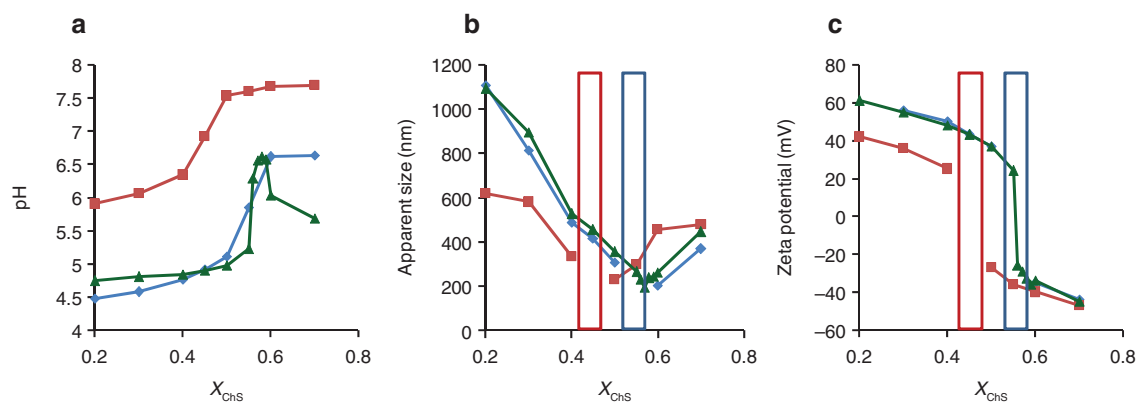


Fig. 2: Final pH (a), apparent hydrodynamic diameter (b), and zeta potential (c) as a function of the X_{ChS} of CS/ChS colloidal suspensions made by sequentially pouring into 3.4 mL of water volumes of CS 0.01 M and volumes of ChS 0.01 M at pH: (◆) 5.9 (water), 4.6 (CS), and 6.6 (ChS); (■) 5.9 (water), 5.9 (CS) and 5.9 (ChS); (▲) 5.0 (water), 5.0 (CS) and 5.0 (ChS). The rectangular areas correspond to the appearance of macroprecipitates.

charges, both negative or positive [26, 34]. However, the high electrical neutralization achieved in equimolar mixtures of both CS and ChS polyelectrolytes favors the formation of macroprecipitates. It has been shown in the literature that CS/ChS nanoparticles can be formed in a wide range of relative and absolute concentrations, up to a threshold beyond which only precipitates in the form of large particles appear [11], but in our experience, in addition to nanoparticles, the appearance of macroprecipitates could not be avoided when pouring a ChS solution to a CS solution at conditions near neutrality and pHs 4–7. We have performed experiments in which the total concentration of polymeric ionizable groups, both acid and basic, was set at 4.44×10^{-3} M, showing variable relative composition of both polysaccharides. The mixtures were prepared by pouring solutions of ChS to solutions of CS, varying the volumes of both CS and ChS stock solutions, following the sequential method introduced in the experimental part. The results concerning the final pH achieved, the apparent hydrodynamic diameter, and the zeta potential are shown in Fig. 2 as a function of the ChS molar fraction (X_{ChS}).

ChS carboxylate units deprotonate at pHs in the range between 3 and 6, and CS ammonium groups deprotonate at pHs in the range between 5 and 8. The respective stock solutions prepared spontaneously achieved pH 6.6 and 4.6. By mixing different amounts of both stock solutions without further pH adjustment, the pH of the resulting mixtures took values ranging between 4.5 and 6.5, as can be seen in Fig. 2a. Most of the mixtures acquired a milky appearance related to their colloidal nature. The corresponding apparent particle size and zeta potentials are shown in Fig. 2b and c. The values of the PDI concerning their apparent size ranged between 0.15 and 0.30, revealing a monomodal distribution of the particles. At low X_{ChS} the resulting pH is low enough to induce a decrease on the total ChS charge, thus, interaction with excess of CS produces large particles (Fig. 2b) showing a high positive zeta potential (Fig. 2c). As the X_{ChS} increases, the pH increases as well as the total polymeric negative charges, whereas the amount of positive charges of CS decreases, thus producing smaller particles with still positive zeta potential, high enough to ensure stability of the colloids up to X_{ChS} of almost 0.5, at pH 5.0. However, near the electroneutralization point, the mixture underwent precipitation, as can be seen in Fig. 3 and signaled by the square areas in Fig. 2b and c. This occurred at X_{ChS} of 0.55 and pH 5.9. From X_{ChS} of 0.6 the pH achieves a value of 6.5, particles of 200–400 nm are formed, and the zeta potential is inverted, witnessing the excess of negative charges in the mixtures where in addition to the excess of ChS, some of the CS ammonium groups have lost their charges. Based on the results of these experiments, other experiments were performed in which the pH of both polysaccharide stocks solutions and water was previously adjusted to 5.9. In these experiments, the interaction between both polysaccharides consumed protons from water, as can be deduced by the significant increase on the pH with the increase on the X_{ChS} shown in Fig. 2a. Indeed, the negative charges of ChS should stabilize the positive charges of CS, so that the partially deprotonated CS protonates. Thus, the electroneutralization point and consequent precipitation

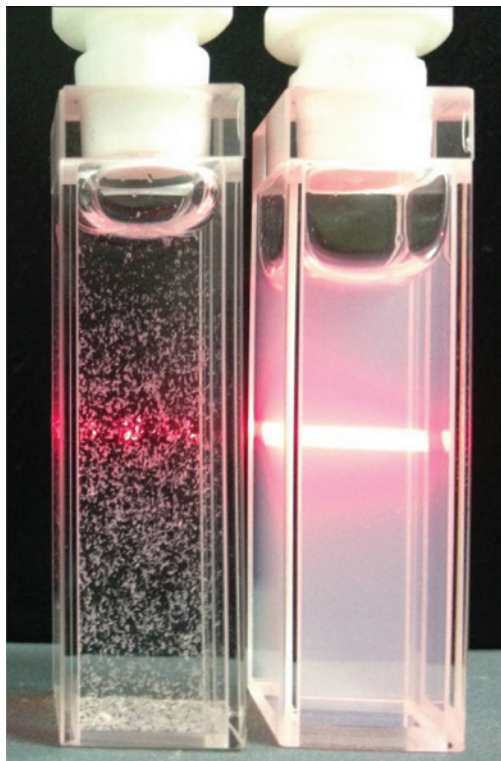


Fig. 3: Left: precipitate mixture of CS and ChS at X_{chs} of 0.55 (pH 5.9) prepared by the sequential method without previous pH adjustment of precursor stock solutions; right: colloidal suspension of CS/ChS nanoparticles at X_{chs} of 0.55 (pH 5.6) prepared by the simultaneous method. The suspensions are traversed by a laser beam.

occurred at X_{chs} of around 0.45 and pH 6.9. At lower X_{chs} colloidal suspensions are formed showing positive zeta potential, and at higher X_{chs} the colloidal suspensions formed presented negative zeta potential. Near the electroneutrality, the colloidal suspensions are smaller, and in all cases the PDI of the colloids ranged between 0.18 and 0.35. Interestingly, if the pH of both polysaccharide stocks solutions and water is adjusted to 5.0, the corresponding mixtures followed trends very similar to those obtained when the pH was not previously adjusted to any fixed value, but macroprecipitates do not appear at the electroneutralization point, also occurring at X_{chs} of around 0.55, as seen by the inversion of the zeta potential. The PDI concerning the apparent size of the colloidal suspensions ranged between 0.14 and 0.29, revealing the good quality of the colloids. The final pH of the colloidal suspensions stands a little lower than 5.0 up to a X_{chs} of around 0.55, witnessing the release of protons of the partially protonated ChS, as CS positive charges stabilize the negative charges of the polyanion; then the pH jumps up to 6.5, revealing that the excess of ChS induces CS further protonation. From a X_{chs} of around 0.6, the excess of ChS stock solution at pH 5 induces a further decrease on the pH. In addition, we have made experiments to overcome macroprecipitation at the electroneutralization point in the case where no previous pH adjustment of the stock solutions or water was made, by changing the mixture protocol. By simultaneously pouring the CS and ChS stock solutions in a flask containing water at pH 5.9, following the simultaneous method described in the experimental part, colloidal suspensions of X_{chs} of 0.55 were obtained showing an apparent size of 206 nm (PDI of 0.15), positive zeta potential of 22 mV, and final pH of 5.6. The resulting colloidal suspension can be seen in Fig. 3 as a milky suspension.

We can explain these results considering the mixing of the stock solutions as an out-of-equilibrium process in which protonation and deprotonation of molecular segments occur during the ionic assembling of the different components, which may include associations by hydrogen bonds and hydrophobic forces of the polysaccharides. This has been observed in other systems, in which during the mixture of stock solutions presenting different pHs, rearrangement of the molecular system produces nanoparticles which are not formed at the equilibrium [35]. In addition, due to the large amount of charges of each single polymeric chain, once

the molecules bind each other, they do not detach easily. Factors that influence the particle size and PDI of the formulations during the out-of-equilibrium process of mixing may be size of the container, final volume, stirring speed, simultaneity and speed of the addition, temperature, pH of the polymeric stock solutions and of the mixture in the container, relative and absolute concentration of the polymers, and the presence of other species in the mixture. In this sense, the presence of acetic acid, where CS is normally dissolved to prepare formulations and scaffolds, could jeopardize the formation of colloidal suspensions at the same conditions used here, affecting the final biological properties. Summarizing, here we have seen the strong influence of the pH and the addition protocol on the formation of colloidal suspensions of both polysaccharides near the electroneutralization point. Colloids of smaller apparent size are found at X_{ChS} close to which the system collapses and produces macroprecipitates. In addition, macroprecipitation at the electroneutralization point could be avoided by adjusting all solutions to pH 5.0 prior to mixing following the sequential method of synthesis, or simultaneously mixing both polysaccharide stock solutions without previous adjustment of the pH if the simultaneous method is used.

Aerogel formation

Upon freezing the colloidal suspension of the polysaccharide nanocomplexes obtained near the electroneutralization point by the simultaneous method, or those obtained by the sequential method after pH adjustment to 5.0, the nanometric particles are concentrated during ice formation at the boundary of ice crystals, submitted to the so-called “ice-segregation-induced self-assembly” (ISISA) [36–38]. Electrostatic interactions between the complementary charged chains of CS and ChS and their rigidity enhance the cohesive forces between particles. Sublimation of ice crystals during freeze-drying allows, then, obtaining well-structured porous materials. The sugar-cotton-like porous aerogels, of total mass of 2.2 mg, presented quasi-cylindrical shapes of 12 mm of diameter, slightly lower than the wells used for their production, and rounded edges, as can be seen in Fig. 4. In addition, during the sublimation step the materials expand in the z axis, showing heights of 3–6 mm and density ranging between 3.1 and 6.4 mg/cm³. According to our experience, the density of the aerogels varies with the dimensions of the container and the volume of liquid added, magnitudes critical for the extent of contraction in the x/y plane and expansion in the z axis. SEM images of the aerogels are shown in Fig. 5. The materials are composed of microsheets and microfibers presenting a smooth surface.

Assays of measuring the porosity of the aerogels in a pycnometer failed, since the low volume displaced by the solid part of the materials fell in the error range of the equipment. The volume of the solid part of the

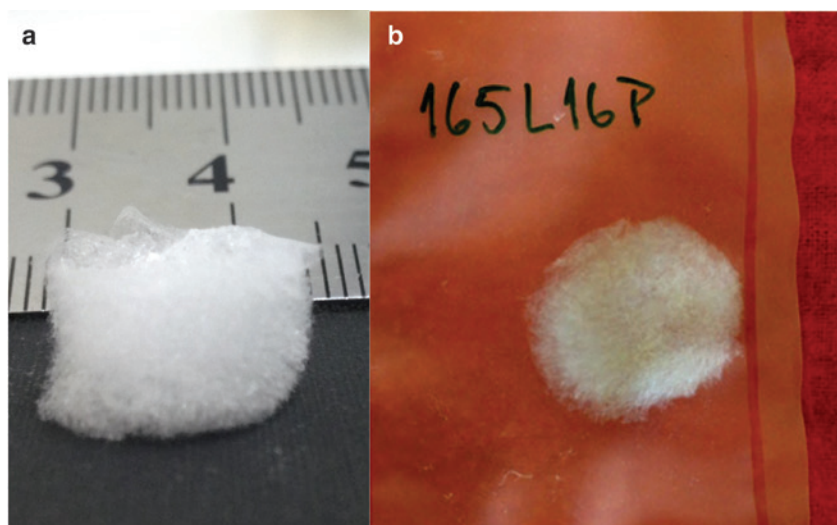


Fig. 4: CS/ChS aerogel after freeze-drying (a) and compressed, sterilized, packed and labeled for storage and transportation (b).

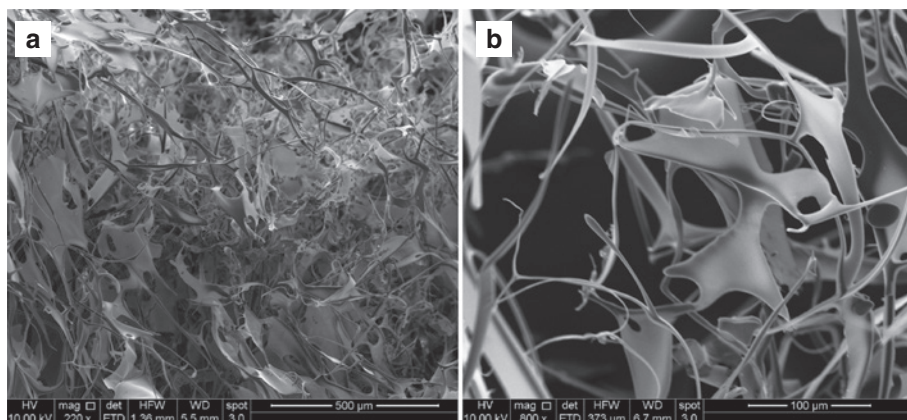


Fig. 5: SEM images of CS/ChS aerogels at two different magnifications: 220 \times (a), 800 \times (b).

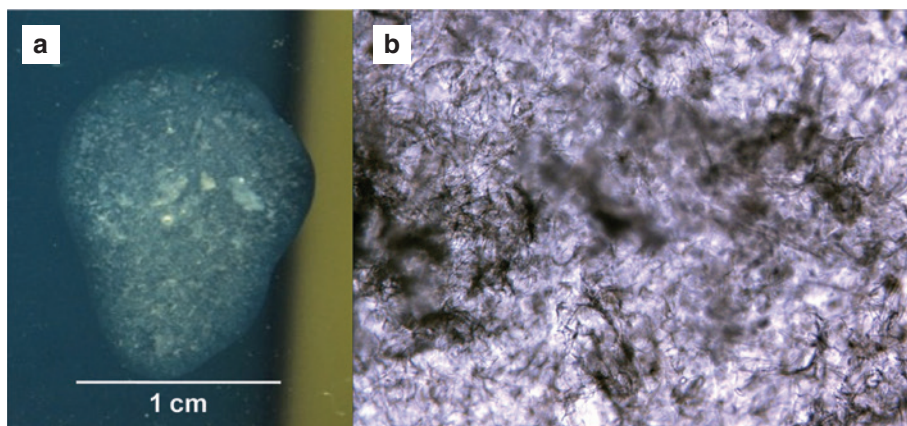


Fig. 6: Images taken at naked eye (a) and by optical microscopy (4 \times) (b) of CS/ChS aerogels of 12 mm of diameter after addition of 100 μ L of water.

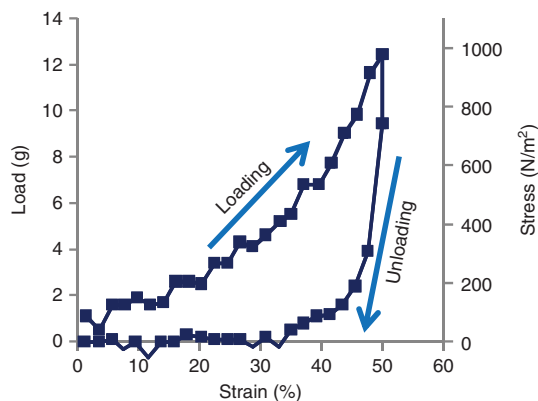


Fig. 7: Typical strain-stress behavior of the aerogels investigated.

materials, and thus a threshold of porosity, could be estimated assuming that the microsheets and microfibrers of the aerogels are slightly denser than the low-dense organic solvent cyclohexane, as the aerogels did not show floatability in it. A total maximum volume of 2.8 mm³ is obtained for the solid part of the aerogels, as calculated taking the density of cyclohexane (779 mg/cm³ at 20 °C) as the lower limit density. By comparison

with the experimentally minimum volume found for well-formed aerogels, i.e. 339 mm^3 , porosity higher than 99 % is theoretically calculated, even considering an error of 15 % on the estimation of the volume of the aerogel.

Upon addition of a small amount of water to the aerogels the microstructures slightly swell, and the material hydrates and slowly disperses in small pieces, as can be seen in Fig. 6. However, the compressed, sterilized, packed form of the material (Fig. 4b), applied to low exudative skin lesions, hydrates and forms a hydrogel that adheres to the injured skin [18].

We observe by compression analyses that the aerogels have low stiffness. Their stress-strain curves show a nonlinear behavior with viscoelastic characteristics. An example is given in Fig. 7. Hardness of around 12 g was obtained at 40–50 % deformation ($n = 5$). The E_{app} analysis obtained from the stress-strain curves in the range of 30–50 % deformation gave values of $2.2 \pm 0.3 \text{ kPa}$ ($n = 5$), far beyond the lower bound of the expected values for flexible foams [39], a fact that is related to the low density and high porosity of the materials.

Final remarks

Ultralight, low-dense CS/ChS aerogels are materials with high potential in wound healing of chronic wounds such as diabetic foot and venous ulcers. Applied to the skin lesions, they improve the quality of the dermal tissue, with suppression of pain and accelerating wound healing, as has been previously corroborated by our research group [18]. After applied in the open wound, the material swallows and hydrates, adhering to the injured skin, so that it does not need to be removed, since it is physiologically degraded. In the case of venous ulcers, to control the exudates usually absorbent dressings are used. The low density of the materials minimizes the chances of adverse reactions. Indeed, it is recognized that low-dense biomaterials present better biological properties for several applications [29], since denser materials that must be physiologically degraded by the patient may involve higher metabolic stress in the damaged tissue, producing debris and by-products of metabolism, providing nutrients and factors for bacteria adherence, colonization and growth. The therapeutic potential of these materials as healing inductors is based on their angiogenic properties related to the biological action of both CS and ChS polysaccharides.

Here we show a simple and low-cost production protocol that avoids chemical reactions producing covalent bonds and the use of organic solvents. The simplicity of the formulation, containing low mass and avoiding the use of stem cells or exogenous proteins, thus minimizing the risk of hypersensitivity reactions, is an advantage of this material. Additionally, easiness of production, storage, and transportation reduces associated costs. The originality of the formulation stems on the conception of the assembling process as an out-of-equilibrium process, so that carefully tuning the variables during mixing and freeze-drying allowed obtaining functional materials that accomplish the requisites of showing low density, being composed of biologically active molecules, and presenting minimum excess of any charged polymeric component.

The obtained materials are light and soft. Their mechanical properties facilitate their application in open wounds, easily adapting to the wound contour due to their low toughness and hydration ability. In addition, they can be easily compressed, sterilized and packed in appropriate containers, as can be seen in Fig. 4b, thus facilitating their storage and transportation, conditions necessary for their adequate commercialization and clinical management.

Conclusions

CS/ChS aerogels have been fabricated as biomaterials designed for wound healing. The production protocol was conceived following three major requirements: (1) the biomaterial should be ultralight and porous; (2) the biomaterial should be functional; (3) the biomaterial should present low electrical potential. As a first step of fabrication, colloidal suspensions of CS/ChS nanocomplexes have been produced in water. The

major challenge of avoiding macroprecipitation in almost equimolar mixtures of both polysaccharides has been overcome by simultaneously mixing stock solutions of the polysaccharides without any pH adjustment before mixing, and by sequentially mixing stock solutions previously adjusted to pH 5.0. The solid materials, made after solvent removal from the colloidal suspensions, present density in the order of 10^0 – 10^1 mg/cm³, and porosity higher than 99 %, and a porous structure consisting of a network of microfibers and microsheets. Their mechanical properties allow their compression, easy packing, storage, transportation and application in open wounds. The easy to handle engineered materials provide potential application in chronic skin lesions.

Acknowledgments: This work was supported by FONDECYT Regular (grants no. 1150899 and 1161450), FONDECYT Iniciación (grant no. 11150919), Fondecyt Postdoctorado (grant no. 3110153), CONICYT-FONDAP 15130011, and Gobierno Regional de Los Ríos (grants FIC-R-2011 and FIC-R 2012-117).

References

- [1] H. Maleki, L. Durães, C. A. García-González, P. del Gaudio, A. Portugal, M. Mahmoudi. *Adv. Colloid Interface Sci.* **236**, 1 (2016).
- [2] K. S. Mikkonen, K. Parikka, A. Ghafar, M. Tenkanen. *Trends Food Sci. Technol.* **34**, 124 (2013).
- [3] C. A. García-González, M. Alnaief, I. Smirnova. *Carbohydr. Polym.* **86**, 1425 (2011).
- [4] R. M. Rajendar, A. M. Michael, S. Vasudha, S. Bano, R. R. Raj, C. K. Subhas, A. M. Mark. *Biomed. Mater.* **10**, 035002 (2015).
- [5] N. Nwe, T. Furuike, H. Tamura. *Materials* **2**, 374 (2009).
- [6] Y.-G. Ko, N. Kawazoe, T. Tateishi, G. Chen. *J. Biomed. Mater. Res. Part B Appl. Biomater.* **93B**, 341 (2010).
- [7] C. Matschegewski, J.-B. Matthies, N. Grabow, K.-P. Schmitz. *Curr. Opin. Biomed. Eng.* **2**, 11 (2016).
- [8] M. Rodríguez-Vázquez, B. Vega-Ruiz, R. Ramos-Zúñiga, D. A. Saldaña-Koppel, L. F. Quiñones-Olvera. *BioMed Res. Int.* **2015**, 15 (2015).
- [9] S. Stratton, N. B. Shelke, K. Hoshino, S. Rudraiah, S. G. Kumbar. *Bioact. Mater.* **1**, 93 (2016).
- [10] K. Sugahara, H. Kitagawa. *Curr. Opin. Struct. Biol.* **10**, 518 (2000).
- [11] M.-K. Yeh, K.-M. Cheng, C.-S. Hu, Y.-C. Huang, J.-J. Young. *Acta Biomater.* **7**, 3804 (2011).
- [12] A. B. Souza-Fernandes, P. Pelosi, P. R. Rocco. *Crit. Care* **10**, 237 (2006).
- [13] N. Afratis, C. Gialeli, D. Nikitovic, T. Tseggenidis, E. Karousou, A. D. Theocharis, M. S. Pavão, G. N. Tzanakakis, N. K. Karamanos. *FEBS J.* **279**, 1177 (2012).
- [14] A.-R. Im, J. Y. Kim, H.-S. Kim, S. Cho, Y. Park, Y. S. Kim. *Nanotechnology* **24**, 395102 (2013).
- [15] T. Koike, T. Izumikawa, J.-I. Tamura, H. Kitagawa. *Biochem. Biophys. Res. Commun.* **420**, 523 (2012).
- [16] J. S. Park, H. J. Yang, D. G. Woo, H. N. Yang, K. Na, K. H. Park. *J. Biomed. Mater. Res. Part A* **92**, 806 (2010).
- [17] G. Cardenas, P. Anaya, C. von Plessing, C. Rojas, J. Sepulveda. *J. Mater. Sci. Mater. Med.* **19**, 2397 (2008).
- [18] A. Vidal, A. Giacaman, F. A. Oyarzun-Ampuero, S. Orellana, I. Aburto, M. F. Pavicic, A. Sánchez, C. López, C. Morales, M. Caro, I. Moreno-Villoslada, M. Concha. *Am. J. Ther.* **20**, 394 (2013).
- [19] R. Jayakumar, M. Prabakaran, P. T. Sudheesh Kumar, S. V. Nair, H. Tamura. *Biotechnol. Adv.* **29**, 322 (2011).
- [20] S. V. Madhally, H. W. Matthew. *Biomaterials* **20**, 1133 (1999).
- [21] F. Croisier, C. Jérôme. *Eur. Polym. J.* **49**, 780 (2013).
- [22] D. G. Miranda, S. M. Malmonge, D. M. Campos, N. G. Attik, B. Grosogeat, K. Gritsch. *J. Biomed. Mater. Res. B Appl. Biomater.* **104**, 1691 (2016).
- [23] P. X. Ma, J. Elisseeff. *Scaffolding in Tissue Engineering*, CRC Press, Boca Raton, FL (2005).
- [24] R. A. Muzzarelli, F. Greco, A. Busilacchi, V. Sollazzo, A. Gigante. *Carbohydr. Polym.* **89**, 723 (2012).
- [25] A. E. Nel, L. Madler, D. Velegol, T. Xia, E. M. V. Hoek, P. Somasundaran, F. Klaessig, V. Castranova, M. Thompson. *Nat. Mater.* **8**, 543 (2009).
- [26] S. L. Orellana, A. Giacaman, F. Pavicic, A. Vidal, I. Moreno-Villoslada, M. Concha. *J. Biomed. Mater. Res. A* **104**, 2537 (2016).
- [27] A. R. Fajardo, L. C. Lopes, A. J. M. Valente, A. F. Rubira, E. C. Muniz. *Colloid Polym. Sci.* **289**, 1739 (2011).
- [28] A. R. Fajardo, J. F. Piai, A. F. Rubira, E. C. Muniz. *Carbohydr. Polym.* **80**, 934 (2010).
- [29] K. C. Kavya, R. Dixit, R. Jayakumar, S. V. Nair, K. P. Chennazhi. *J. Biomed. Nanotechnol.* **8**, 149 (2012).
- [30] A. Denuziere, D. Ferrier, O. Damour, A. Domard. *Biomaterials* **19**, 1275 (1998).
- [31] A. Bianchera, E. Salomi, M. Pezzanera, E. Ruwet, R. Bettini, L. Elviri. *J. Anal. Methods Chem.* **2014**, 8 (2014).
- [32] J. F. Piai, L. C. Lopes, A. R. Fajardo, A. F. Rubira, E. C. Muniz. *J. Mol. Liq.* **156**, 28 (2010).
- [33] A. R. Fajardo, L. C. Lopes, A. O. Caleare, E. A. Britta, C. V. Nakamura, A. F. Rubira, E. C. Muniz. *Mater. Sci. Eng. C* **33**, 588 (2013).
- [34] K. Jain, P. Kesharwani, U. Gupta, N. K. Jain. *Int. J. Pharm.* **394**, 122 (2010).

- [35] E. Araya-Hermosilla, S. L. Orellana, C. Toncelli, F. Picchioni, I. Moreno-Villoslada. *J. Appl. Polym. Sci.* **132**, 42363 (2015).
- [36] M. C. Gutiérrez, M. L. Ferrer, F. del Monte. *Chem. Mater.* **20**, 634 (2008).
- [37] X. Zhang, C. Li, Y. Luo. *Langmuir* **27**, 1915 (2011).
- [38] L. Sanhueza, J. Castro, E. Urzúa, L. Barrientos, F. Oyarzun-Ampuero, H. Pesenti, T. Shibue, N. Sugimura, W. Tomita, H. Nishide, I. Moreno-Villoslada. *J. Phys. Chem. B* **119**, 13208 (2015).
- [39] M. F. Ashby. *Materials Selection in Mechanical Design (Fourth Edition)*, pp. 57–96, Butterworth-Heinemann, Oxford (2011).